A Model for Computing and Energy Dissipation of Molecular QCA Devices and Circuits

XIAOJUN MA, JING HUANG, and FABRIZIO LOMBARDI
Northeastern University, Boston

Quantum-dot Cellular Automata is an emerging technology that offers significant improvements over CMOS. Recently QCA has been advocated as a technology for implementing reversible computing. However, existing tools for QCA design and evaluation have limited capabilities. This paper presents a new mechanical-based model for computing in QCA. By avoiding a full quantum-thermodynamical calculation, it offers a classical view of the principles of QCA operation and can be used in evaluating energy dissipation for reversible computing. The proposed model is mechanically based and is applicable to six-dot (neutrally charged) QCA cells for molecular implementation. The mechanical model consists of a sleeve of changing shape; four electrically charged balls are connected by a stick that rotates around an axle in the sleeve. The sleeve acts as a clocking unit, while the angular position of the stick within the changing shape of the sleeve, identifies the phase for quasi-adiabatic switching. A thermodynamic analysis of the proposed model is presented. The behaviors of various QCA basic devices and circuits are analyzed using the proposed model. It is shown that the proposed model is capable of evaluating the energy consumption for reversible computing at device and circuit levels for molecular QCA implementation. As applicable to QCA, two clocking schemes are also analyzed for energy dissipation and performance (in terms of number of clocking zones).

Categories and Subject Descriptors: B.7.1 [**Integrated Circuits**]: Types and Design Styles—*Advanced technologies*; B.8.2 [**Performance and Reliability**]: Performance Analysis and Design Aids; B.6.3 [**Logic Design**]: Design Aids—*Simulation*

General Terms: Theory, design

Additional Key Words and Phrases: QCA, reversible computing, thermodynamic analysis, emerging technology

ACM Reference Format:

Ma, X., Huang, J., and Lombardi, F. 2008. A model for computing and energy dissipation of molecular QCA devices and circuits. ACM J. Emerg. Technol. Comput. Syst. 3, 4, Article 18 (January 2008), 30 pages. DOI = 10.1145/1324177.1324180 http://doi.acm.org/10.1145/1324177.1324180

Authors' address: email: {xma,hjing,lombardi}@ece.neu.edu

1. INTRODUCTION

CMOS is fast approaching its limitations as predicted by the end of the technology roadmap. As alternative for attaining high computational power and compact design density, so-called *emerging technologies* have been the focus of extensive research. Computation at nano regimes is substantially different from conventional VLSI. Extremely small feature size, high device density and low power are some of the attributes that emerging technologies must address, while implementing new computational paradigms [Compano et al. 2005].

One of the most pressing hurdles in the development of innovative computation paradigms and systems is energy dissipation [Lent et al. 2006] because it affects system design as well as devices and circuits. An extensive investigation of the relation between energy dissipation and computing at logic level has been pursued [Bennett 2000] with respect to the thermodynamic limit of computation. Reversible computing has been proposed to avoid this limit and improve computing power without resulting in an unacceptable energy dissipation.

The relation between computing and energy dissipation was initially investigated by Landauer, who showed that $kTln2$ joules of energy are generated for each bit of information lost due to the nonreversibility in the computational process [Landauer 1961] (where k is Boltzmann's constant and T is the operating temperature). Moreover, if computation is performed in a reversible manner, it has been shown that $kTln2$ energy dissipation would not necessarily occur. In reversible computing, the input state of a device can always be uniquely established from its output state (one-to-one onto mapping). This avoids the irreversible process in computation, thus making possible at least in theory to build computational systems, whose energy dissipation is only determined by the number of inputs and outputs, not by the number of gates in the system. For a large system, the amount of energy per gate can be made very small, so that the high density integration of systems manufactured in the nano-scale will not be limited by energy dissipation.

Among emerging technologies, *Quantum-dot Cellular Automata* (QCA) [Lent et al. 1994; Smith 1999] relies on novel design concepts to exploit physical phenomena (such as Coulombic interactions). It can implement unique paradigms with desirable features, such as low power [Frost et al. 2002; Niemier and Kogge 2001]. QCA has been deemed as a promising technology for approaching the thermodynamic limit of computation and building reversible logic systems. Several QCA models have been proposed for different QCA implementation technologies [Tougaw and Lent 1994; Tang et al. 2005; Lent et al. 2006]. The model in Lent et al. [2006] has also been applied to analyze energy dissipation in QCA; Lent et al. [2006] and Timler and Lent [2003] have shown by quantitative calculation that it's possible to build reversible logic circuits using QCA.

However, the analysis of reversible logic in the context of QCA requires a substantial content of quantum dynamics. An intuitive understanding of the computational procedure and related energy dissipation is often difficult to

acquire due to the unique features of the quantum effects in QCA. For example, robustness to thermal effects must consider the repeated estimates of ground (and preferably near-ground) states, along with cell polarization for different designs. This evaluation is currently possible only through a full quantum-mechanical simulation. Existing tools such as AQUINAS [Tougaw and Lent 1996] and the coherence vector simulation engine of QCADesigner [Walus et al. 2003] perform an iterative quantum mechanical simulation (using the Hartree-Fock approximation) to calculate the ground state. Other techniques such as QBert [Niemier et al. 2000], Fountain-Excel simulation, nonlinear simulation [Walus et al. 2003] only estimate the state of the cells; in some cases unfortunately, they may fail to estimate the correct ground state. A new model based on a SPICE model has been proposed and experimentally verified in Tang et al. [2005a, 2005b]. Such model characterizes the behavior of metal-based QCA by electrical elements. A metal-island QCA cell is modeled as a network consisting of capacitors, resistors and voltage sources. However, this model does not fully capture the behavior of a QCA cell, as energy and related effects (such as dissipation) are not analyzed. Presently, CAD tools for QCA (such as QCADesigner and AQUINAS) are inadequate in assessing energy dissipation as related to using QCA for reversible computation. Moreover, they are applicable to an evaluation of QCA circuits under specific conditions in clocking scheme and technology implementation.

A mechanical model inspired by the operational features of molecular QCA is proposed in this paper. The main motivation for introducing this new model is that it provides an intuitive and classical treatment of energy and heat phenomena in QCA technology. Based on this model, reversibility of QCA is investigated in detail at both device and circuit levels. QCA devices and circuits are considered. Using this model, different features of QCA devices and circuits are analyzed. For example, the fanout connection is shown to be compatible with the reversible computing paradigm. Also, Landauer and Bennett clocking techniques [Lent et al. 2006] are briefly analyzed to unify reversibility within a cohesive framework for different QCA devices (such as the majority voter). The proposed model has the ability to evaluate different features of QCA circuits (such as clocking scheme, energy calculation and logic state). The proposed mechanical model is currently being used as part of a CAD tool for evaluating molecular QCA; this tool is under development.

This article is organized as follows: Section 2 deals with preliminaries inclusive of a brief review of reversible computing and QCA technology. Section 3 presents in detail the proposed mechanical model, including a steady state analysis of QCA devices. In Section 4, the relationship between entropy and energy dissipation is explored and exploited to present in detail the operation of a model cell. This analysis is then extend to small QCA circuits. Circuits such as the two-cell signal path, shift registers, fanout and three-cell inverter are considered. Clocking schemes (as related to QCA) and energy analysis are presented in Section 5. As an example, the operations of a circuit based on the mechanical model under Bennett and Landauer clocking schemes are outlined. Discussion and conclusions are given in Section 6.

2. PRELIMINARIES

2.1 Reversible Computing

Landauer [1961] has proved that the lower bound of heat dissipation is related to the loss of one bit of information during computation and is on the order of kT. Dissipation can be avoided if computation is carried out with no loss of information (this process is generally known as *reversible computing*). Formally, a *dynamical system* is reversible if from any point of its state set, it is possible to *uniquely trace* a trajectory backward as well as forward in time for its computation [Toffoli 1980]. For any thermodynamical process involving a system moving from state A into state B, the change of entropy is defined by the second law of thermodynamics as

$$S(B) - S(A) \geq \int_A^B \frac{dQ}{T},$$

where $S(A)$ and $S(B)$ are the entropy of a system in state A (initial) and B (final) respectively, and dQ is the infinitesimal amount of heat received by the system at temperature T during the change (from state A to B). The equality sign holds for a *thermodynamically reversible* process. The time reversion of a thermodynamically reversible process also satisfies the above inequality. So, to rewind a reversible process (i.e., to repeat the process from the end to the beginning in reverse order, or from B to A) does not violate the second law of thermodynamics. For a process under constant temperature, reversibility means that the total heat exchange with its environment is $T \times (S(B) - S(A))$. If this process starts and ends at the same state (i.e., a *cycle* is said to occur), then the total exchange is 0. If the cycle is not reversible, the total heat exchange is less than 0; that is, the system is dissipative.

Landauer [1961] has shown that a computation process that loses information, cannot be thermodynamically reversible. So, a computing system must dissipate heat if its working cycle consists of an information loss. To preserve information, primitives in reversible computing must have a *one-to-one onto mapping* between inputs and outputs. This property is called the *bijective property*; primitives with this property are *logically reversible* (or invertible) primitives. The implementations of logically reversible primitives are called *reversible logic gates*, but in most cases these two words are interchangeable; that is, reversible computing is based on invertible primitives and composition rules that preserve invertibility [Toffoli 1980].

Bennett [1973], Toffoli [1980], and Fredkin and Toffoli [1999] have shown that general computation can be accomplished through a logically reversible process (i.e., without destroying, or losing information). Different theoretical models of reversible computing have been proposed in the technical literature [Bennett 2000]. Reversibility can be analyzed in two respects:

(1) *Logic Reversibility:* the bijective property (one-to-one onto function) between the input and output logic states holds. This is independent of the technology and the internal structure of the circuit.

(2) *Thermodynamic Reversibility:* no energy is dissipated. In this case, the internal structure of the circuit must satisfy strict reversible primitives in a given technology as an implementation platform.

Note that thermodynamic reversibility requires logic reversibility; however, a circuit can be logically reversible, but not thermodynamically reversible. In the discussion of this paper, "reversible" means thermodynamically reversible, unless otherwise specified.

2.2 Analysis of a General Computing System

In a computing system, the degrees of freedom of its components are encoded to bear information. A thermodynamic model of a single ideal-gas molecule is presented in this section. Its operation is analyzed in terms of information, entropy and dissipation. By analogy, the relation between entropy change and heat dissipation derived in this model is used in the analysis of the operation and dissipation of the computing model proposed in Section 3.

System entropy increases during loss (or destruction) of information. According to thermodynamics [Fermi 1956], the change of system entropy is $\Delta S = k \ln \frac{W_f}{W_i}$, where k is Boltzmann's constant, W_i and W_f are the number of possible sub-states in the initial and final states, respectively. Q is the heat that the system absorbs from the environment and W is the work done by the system.

For example, an ideal gas has six degrees of freedom (three dimensions of space position and three directions of momentum). If a gas with N_A molecules changes its volume from V_i to $V_f = 2V_i$ in an isothermal expansion, then the change of its entropy is given by $\Delta S = k \ln(V_f^{N_A}/V_i^{N_A}) = N_A k \ln(2)$. Isothermal expansion is reversible [Fermi 1956], so this increase in entropy comes from the heat absorbed from the environment and $Q = \Delta S \times T = N_A \times kT \ln 2$ (Q is positive when the heat goes from the environment to the system). The internal energy of a gas is constant in an isothermal expansion, so the work $W = -Q$ is done to the gas (W is positive when work is done to the system). If the change in volume is achieved by free expansion, then there is no work done in the process; that is, $W = 0$. The internal energy of the system does not change. So, there is no heat exchange between the system and the environment, $Q = \Delta E_{internal} - W = 0$. Free expansion is not reversible, so the change of entropy ΔS is larger than $\int \frac{dQ}{T} = \frac{Q}{T} = 0$.

In a computing system, some degrees of freedom can be used to encode information. So, with no loss of generality, a bistate computing unit divides all possible states into two subspaces, according to the information-bearing degrees of freedom. Consider again the example of an ideal gas; if a gas molecule in a cell (container) with volume $2V$ is utilized as a bistate unit, then information can be encoded by defining a first state as 1 if the molecule is in the upper half of the cell, and a second state as 0 if the molecule is in the lower half of the cell (shown in Figure 1). If there is no separation, the gas can move freely in the cell, thus changing the cell state between 1 and 0. Entropy in this free state is denoted by S_0. The state can be set to 1 by moving the bottom to the middle of the cell. Similarly, moving to the top can set the cell to the 0 state. Assume

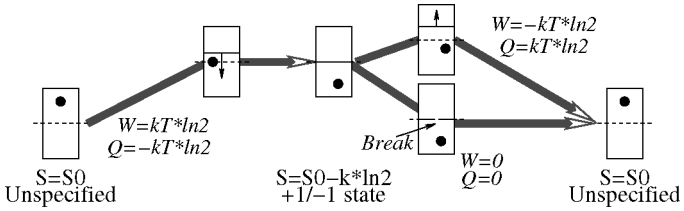

Fig. 1. A memory cell of agas molecule.

the movement is slow enough to keep the operation isothermal, this operation places one bit of information into the cell, and the entropy of the cell becomes $S_0 - k \ln 2$. If the temperature of the system is denoted by T, then $W = kT \ln 2$ of work is done to the cell during the operation, and the heat exchange is given by $Q = -kT \ln 2$.

By knowing the state of a cell, it is then possible to change it from 1 or 0 to the free expansion state by moving the separating wall to the corresponding position (bottom or top). This operation increases the entropy back to S_0; also, $W = -kT \ln 2$ and $Q = kT \ln 2$ are needed for this operation. In the cycle of this process (often referred to as set-then-erase), the total work and heat dissipation are both 0. This is an erasure with no dissipation and can only be performed when the cell state is known. Consider all the parts involved in this operation as a system, rather information is not destroyed in this system. Information will be erased if the separation wall is broken. A molecule's free expansion through the broken wall performs zero work, and the internal energy of the gas experiences no change. So there is no heat exchange between the system and the environment. Meanwhile, the cell entropy increases to S_0 during free expansion. For the working cycle of the set-then-erase operation through free expansion, the work $W = kT \ln 2$ must be done to the system and $Q = -kT \ln 2$ is transferred between the gas (as computing system) and the environment (a negative value means that there is heat dissipation from the system).

This example illustrates that loss of information entails dissipation. Storing information into a logic cell requires heat flow into the environment to decrease the entropy of the cell from the unspecified state. To recover the cell from the unspecified state, it is possible to absorb heat from the environment. The lower limit for the heat generated in the former process is the same as the upper limit of the heat absorbed in the latter process. Both limits are achieved only by a quasi-equilibrium process. The key element of Landauer's claim is that no quasi-equilibrium process can be applied without knowing the state of the information in the system. However, knowledge of information means that the information erased in the cell is not the only copy in the entire computing system; that is, the information is not destroyed. If no other copy of information exists in the computing system, then the above example suggests that the cell can only be recovered to the specified state by a process like free expansion. This process does not absorb heat and the heat dissipation that occurs in the information storage process, is the dissipation of the full work-cycle.

In the above discussion, the base of the logarithm was given by e. The selection of the logarithm base does not change the applicable physical laws that the

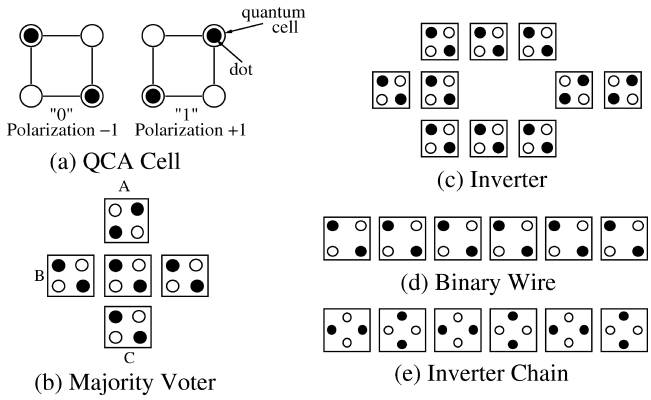

Fig. 2. QCA cell and basic devices.

formula use. As in the remainder of the article, a bistate system is assumed, so a base of 2 will be used to simplify notation and presentation (albeit, also in this case the notation has no implication on the general validity of the presented analysis).

2.3 Quantum-dot Cellular Automata (QCA)

Quantum-dot Cellular Automata (QCA) relies on the Coulombic interaction between cells to implement novel computational paradigms. In its simplest form, a QCA cell can be viewed as a set of four charge containers or "dots" (two dipoles), positioned at the corners of a square [Tougaw and Lent 1994]. The cell contains two extra mobile electrons which can quantum mechanically tunnel between dots, but not cells. The electrons are forced to the corner positions by Coulombic repulsion. The two possible polarization states represent logic "0" (polarization $P = -1$) and logic "1" (polarization $P = +1$), as shown in Figure 2(a). QCA operates by the Coulombic interaction that connects the state of one cell to the state of its neighbors. This results in a technology in which information transfer (interconnection) is the same as information transformation (logic manipulation).

Manufacturing of QCA falls into three major categories of implementation: metal, magnetic and molecular [Toth 2000]. Recent developments in manufacturing involve molecular assembly of QCA devices to supersede metal-based implementations. At very small features sizes, self-assembly and large scale cell deposition on insulated substrates have been proposed [Hu et al. 2005]. In QCA, logic gates (such as the inverter, INV and majority voter, MV) and other devices (such as the binary wire and the inverter chain) have been proposed as primitives for combinational circuit design [Tougaw and Lent 1994]. The basic QCA devices are shown in Figure 2(b)–(e). As a combined methodology for computation and communication [Amlani et al. 1999; Niemier and Kogge 1999; Frost et al. 2002], different designs of logic circuits have been proposed for QCA implementation [Frost et al. 2002; Niemier et al. 2002; Dimitrov et al. 2002; Walus et al. 2002, 2003]. It has been shown [Huang et al. 2005] that for QCA, the function with at most three variables (such as the MV) provides the basis for combinational design.

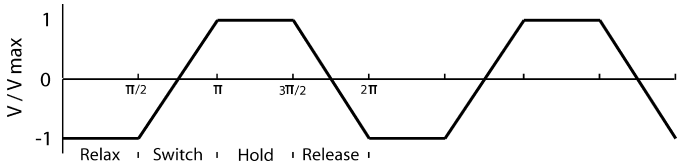

Fig. 3. Four-phased Landauer clocking.

Clocking is used to modulate the inter-dot tunneling barrier of QCA cells. Using an induced electric field mechanism for clocking, true power gain is possible. A QCA circuit is partitioned into a number of clocking zones and all cells in the same zone are controlled by a common clock signal. The clock signals are commonly supplied by CMOS wires buried under the QCA circuitry. The use of a quasi-adiabatic switching technique for QCA circuits requires a four-phased clocking signal. The *four-phase clocking scheme*, also known as Landauer clocking, was proposed by Lent and Tougaw [1997], and is shown in Figure 3. The four phases are RELAX, SWITCH, LOCK, and RELEASE. During the RELAX phase, there is no inter-dot barrier and a cell remains unpolarized. During the SWITCH phase, the inter-dot barrier is slowly raised and a cell attains a definitive polarity under the influence of its neighbors. In the LOCK phase, barriers are high and a cell retains its polarity. Finally in the RELEASE phase, barriers are lowered and a cell loses its polarity. Clocking zones of a QCA circuit or system are arranged in this periodic fashion, such that zones in the LOCK phase are followed by zones in the SWITCH, RELEASE, and RELAX phases. A signal is effectively "latched" when one clocking zone goes into the LOCK phase and acts as input to the subsequent zone. This clocking mechanism provides inherent pipelining [Antonelli et al. 2004] and allows multi-bit information transfer in QCA through signal latching.

QCA has low power consumption, so it has been used as a technology to quantitively investigate the relationship between computation and energy dissipation [Lent et al. 2006; Timler and Lent 2003]. In QCA, the information stored in the cell is "erased" when the cell goes from the LOCK phase to the RELAX phase. Two cases are considered in Timler and Lent [2003]: logically irreversible "erase" and logically reversible "copy-then-erase." Erasure without copying requires an amount of energy dissipation of at least in the order of kT. However, energy dissipation during a "copy-then-erase" process (in which a copy of the bit is retained) can be made arbitrarily small. For a binary wire (such as a QCA shift register), it has also been shown that the energy dissipated per switching operation can be significantly less than $kTln2$. However, it must be pointed out that as the fundamental operation in QCA, the majority voting function is logically irreversible, because the information in the minority input is lost during computation. A novel scheme referred to as *Bennett clocking* has been proposed for QCA in [Lent et al. 2006]. With this scheme, it is possible to build reversible logic circuits for making QCA a realistic technology [Lent et al. 2006] for reversible computing. A detailed treatment of Bennett clocking is discussed in Section 5.

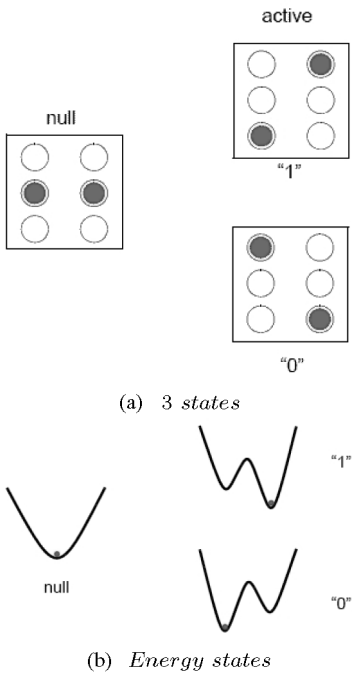

Fig. 4. Tri-state model for clocked molecular QCA.

A tristate model for clocked molecular QCA has been proposed [Lent et al. 2006]. In this model, a QCA cell has 2 electrons and 6 dots, as shown in Figure 4 [Lent et al. 2006]. This cell has three possible charge configurations: when the electrons are in the corner dots, an active state (i.e., either a 0 or a 1 state) is said to be present in the cell; when the two electrons are in the middle dots, this represents a *NULL* state. Tunneling between dots only enables the cell state to switch directly between active states and the *NULL* state. A QCA cell must go through the *NULL* state to switch from one active state to the other active state. The tristate cell is still driven by a four-phase clock. In the RELAX phase, the electrons are forced in the middle dots, so the cell is in the *NULL* state. In the SWITCH phase, the electrons tunnel to the corner dots; so, the cell changes to an active state (either Boolean 1 or 0) according to the configurations of its neighbor cells. In the LOCK phase, tunneling is disabled, so the cell is kept in its active state. In the RELEASE phase, the electrons tunnel back to the middle dots, so the cell is back to the *NULL* state. Figure 5 shows a three dimensional view of a molecular QCA under this clocking scheme [Lent et al. 2006].

3. MECHANICAL MODEL

As a nanoscale device technology, the behavior of molecular QCA can be modeled using a tristate model as proposed by Timler and Lent [2003]. Inspired by Timler and Lent [2003], a novel mechanical model is proposed in this paper for the analysis of energy and the reversible features of logic design.

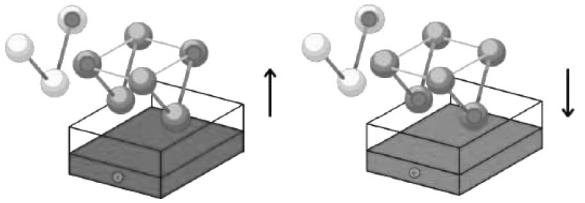

Fig. 5. Clocked molecular QCA.

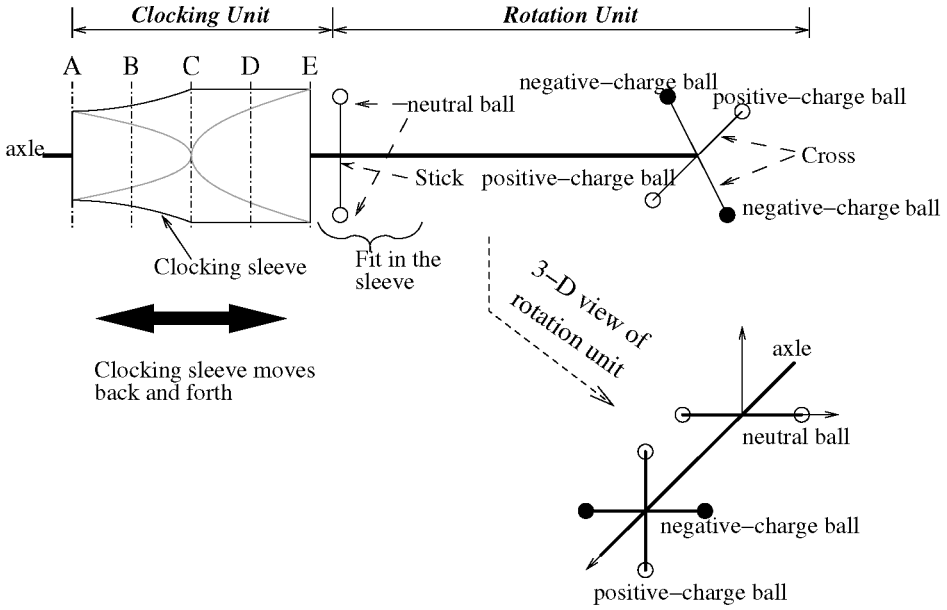

(a) Diagram of a cell of proposed model

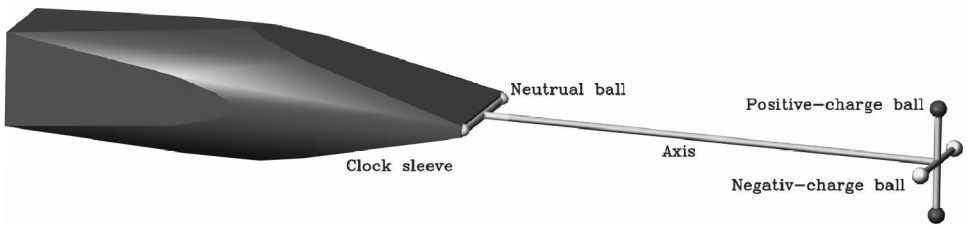

(b) 3D view of a cell

Fig. 6. Mechanical model for molecular QCA.

3.1 Model of QCA Cell

Figure 6 illustrates the computing cell in the proposed mechanical model; as shown in the following sections, it correctly models the logic behavior of QCA devices and circuits. As shown in Figure 6(a), each cell consists of two units: the *rotation unit* and the *clocking unit*. A 3D view of the entire mechanical computing cell is given in Figure 6(b).

—*Rotation unit*: There are four charged balls installed at the end of a cross with four equal-length arms. Two of the balls have positive charge and the other two balls have negative charge. The charged balls are positioned to form a quadrupole, as shown in the 3D view of rotation unit in Figure 6(a). A compressible unbendable stick connects two (neutral) balls. The center of the cross and the midpoint of the stick are installed on the same axle. The cross and the stick are tightly fixed to the axle and are always kept aligned as shown in Figure 6(a). The position of the axle is fixed, so the only possible movement of the rotation unit is rotating around the axle.

The angular position of the rotation unit is used to represent the information in the computing system. The charged balls in different cells interact with each other through a Coulomb force. The quadrupole interaction between mechanical computing cells can model the quadrupole interactions between cells in molecular QCA. The interaction among the mechanical computing cells is used to transfer and transform the information, in a way similar to the information processed in QCA circuits.

—*Clocking unit*: The neutral balls are housed in a specially shaped sleeve. The cross section of the sleeve has different shapes at different positions. Figure 7(a) illustrates the cross sections generated by cutting at the five positions (A)–(E) of Figure 6(a). The forth-and-back movement of the sleeve changes the shape that contains the neutral balls.

The possible angular position of the rotation unit (denoted by β in Figure 7) is limited by the shape of the cross section of the sleeve. A large amount of energy with be required for pressing the neutral balls into the narrow part of the sleeve. This will also compress the stick connecting the balls. Thus, the position of the sleeve defines the energy state with respect to β. The plot of the energy state versus β (at the sleeve position denoted by (A)–(E)) is shown in Figure 7(c). The position of the charge-ball quadrupole corresponds to the degree of freedom used to encode information; this is shown under the five different scenarios in Figure 7(b). The sleeve interacting with the neutral balls defines the clocking operation in the computing model, hence it is referred to as the *clocking unit*. The clocking unit works as the electrical field for QCA clocking—the electrical field also changes the energy profile of the QCA cell with a change in clocking phases. Both sleeve-clocking and QCA-clocking operate by limiting the state transitions of the cells.

The model uses a four-phase clock configured similarly to the four-phase clock of QCA. In the LOCK and RELAX phases (corresponding to state (A) and (E) in Figure 7), the model precisely captures the energy state configuration of a QCA cell. In the LOCK phase, the clock sleeve constrains the angular position β of the rotation unit into two possible polarizations, 45° and 135°. Any other angular position requires the stick to be compressed to fit in the sleeve. As shown in Figure 7(c), the energy for compressing the stick causes the energy for the position to raise rapidly when the angular position deviates from 45° or 135°. Like a QCA cell, in which electrons can only be in state "1" or "0" during the LOCK phase, the rotation unit in the proposed cell is only allowed to be in a tight range close to 45° and 135°. According to β , the two polarizations are

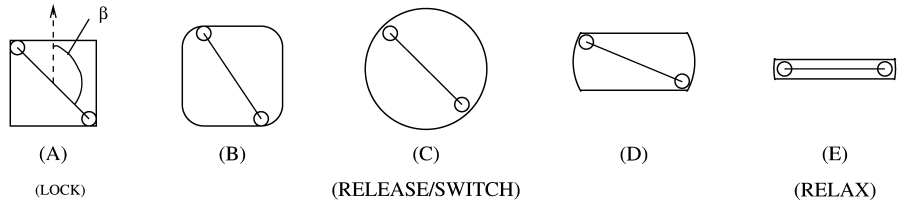

(a) Cross–section of the clocking sleeve

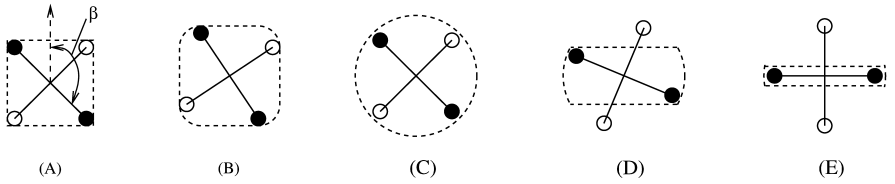

(b) Position of charged balls

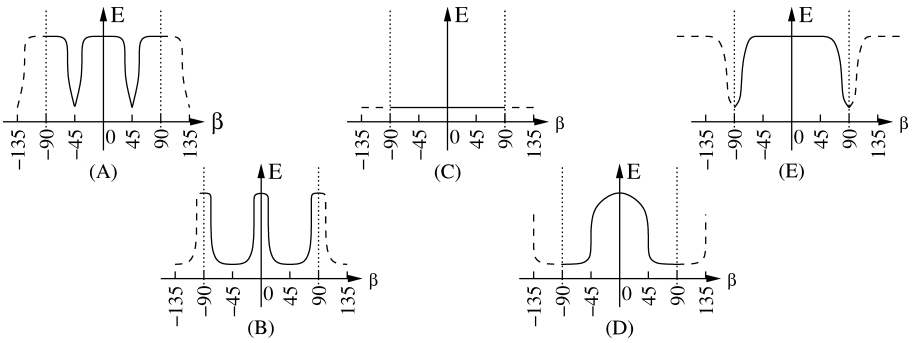

(c) Energy vs angular position

Fig. 7. Clocking of the proposed model.

referred to as state 1 ($\beta = 45^\circ$) and 0 (135°). In the RELAX phase, the rotation unit is allowed to be in a wide range around $\beta = 90^\circ$. This state represents the "NULL" state in a tristate molecular QCA cell.

States (B)–(D) correspond to the SWITCH or RELEASE states in QCA. In state (C), the rotation unit is free to rotate to any angular position. It represents the state of a QCA cell in which the electrons can tunnel freely to any position. The states (B) and (D) are the transitions from (A) to (C) and (C) to (E). The rotation unit can move freely only within an angle defined by the round part shown in the sleeve's cross sections.

It is assumed that the change of the clock (as corresponding to the movement of the sleeve) is slow enough to ensure that *quasi-adiabatic switching* is applicable to the operation of the model [Landauer 1961]. The mechanical computing cell is filled with air, so the air behaves as a damper if the movement of the charged balls is not sufficiently slow (note that air is just a medium in the model, not a physical requirement for molecular implementation). Also, air

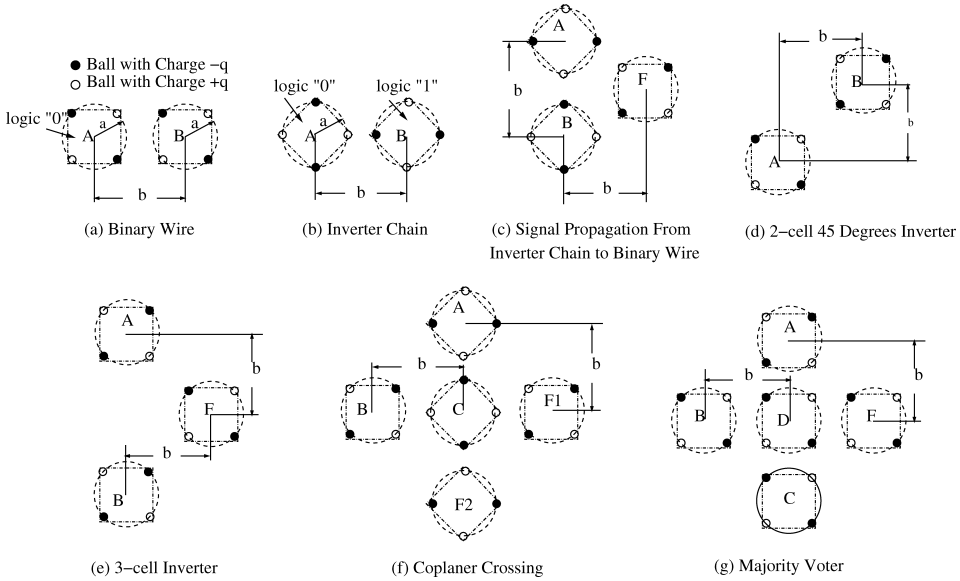

Fig. 8. Steady State Analysis of QCA Devices.

is a source of thermal noise that gives the charged balls a random "Brownian" rotation movement.

3.2 Steady State Energy of QCA Devices

A QCA circuit operates by mapping the ground state to the logic solution that the circuit is designed to generate [Lent Tougaw 1997]. In this section, the steady state energy is calculated for several QCA devices/circuits under the proposed model. The analysis shows that the proposed model agrees with the operation of all basic QCA devices.

Assume that the size of a cell is $a \times a$; the cell center-to-center distance is denoted by b. Hereafter, it is assumed that $b = 3a$. An electric potential energy is associated with interacting charges [Fermi 1956]. Let two electrically charged balls in each cell be viewed as a point charge. Each positive ball has a charge $q_1 = q$, and each negative ball has a charge $q_2 = -q$. For each pair of balls at a distance of r, the potential energy is given by $E = \alpha \times q_1 q_2 / r$, where α is Coulomb's constant. To find the potential energy of a system with a set of charges, the energies associated with each pair of charges must be added. It will be shown next that for all QCA devices/circuits, this model correctly captures their operation; that is, the lowest energy configuration corresponds to the expected function.

Binary Wire. The simplest circuit in QCA is the two-cell binary wire, as shown in Figure 8(a). A is the input, while B is the output. The two possible energy states, namely the aligned ($A = 0, B = 0$) and the anti-aligned states ($A = 0, B = 1$) are shown in Table I. Note that by symmetry, the energy of state $A = B = 1$ is the same as the energy of state $A = B = 0$ (also the energy of state $A = 1, B = 0$ is the same as the energy of state $A = 0, B = 1$), therefore

Table I. Steady State Energy of QCA Circuits

Device	Cell State					Energy ($\times \alpha q^2/a$)
	A=	B=				
binary wire	0	0				−3.87
	0	1				−3.44
2-cell inverter chain	A=	B=				
	0	1				−3.99
	0	0				−3.33
+ to x conversion	A=	B=	F=			
	1	0	1			−6.093
	1	0	1			−5.536
2-cell 45 degree inverter	A=	B=				
	1	0				−3.702
	1	1				−3.610
3-cell inverter	A=	B=	F=			
	1	1	0			−5.586
	1	1	1			−5.398
coplanar crossing	A=	B=	C=	F1=	F2=	
	1	1	0	1	1	−9.800
	1	1	0	0	1	−9.786
	1	1	1	1	0	−9.156
	1	1	1	0	0	−9.144
	1	1	1	0	1	−8.470
	1	1	0	0	0	−9.144
	1	1	0	1	0	−9.156
	1	1	1	1	1	−8.483
majority voter	A=	B=	C=	D=	O=	
	1	0	0	0	0	−9.57
	1	0	0	1	1	−9.13
	1	0	0	0	1	−9.13
	1	0	0	1	0	−8.71

the energy of state $A = B = 0$ (also state $A = 1, B = 0$) is omitted in Table I. For this device, the aligned state has the smallest energy. As expected, the two cells in the binary wire tend to have the same polarization.

Inverter Chain. By rotating the cells 45 degrees, a binary wire becomes an inverter chain, as shown in Figure 8(b). The possible energy states are shown in Table I. It can be observed that when input $A = 0$, the lowest energy state is when output $B = 1$; that is, adjacent cells have opposite polarization. This is in agreement with the expected operation of an inverter chain in QCA.

Signal Propagation from an Inverter Chain to a Binary Wire. Some QCA circuits use both the inverter chain and binary wire, this is required for a circuit in which signals can be propagated from an inverter chain to a binary wire (and vice versa). The circuit that propagates a signal from an inverter chain to a binary wire, is also referred to perform a "+" to "×" conversion and is shown in Figure 8(c). A and B are the inputs (A and B are part of the inverter chain) and F is the output (F can then be used to drive a binary wire). Assume $A = 1$ and $B = 0$, then the possible energy states are shown in Table I. The lowest energy state corresponds to the state in which $F = 1$, as expected.

Inverter. In QCA, two cells placed at a 45 degree orientation will anti-align; that is, they have opposite polarization. This structure is referred to as a 2-cell 45 degree inverter, as shown in Figure 8(d), where A is the input and B is the output. Let $A = 0$, then the energy of two cells placed at a 45 degree orientation is calculated using the proposed model, as shown in Table I. From the calculation, the lowest energy state is when $B = 1$, in which the two cells anti-align. By symmetry, it can be shown that when input $A = 1$, the lowest energy state is obtained when $B = 0$. Therefore in the proposed model, the 45 degree cell orientation operates as expected.

Next, consider the three-cell INV, as shown in Figure 8(e). A and B are the fixed inputs for $A = B$; F is the output. Let $A = B = 1$, then two possible energy states ($F = 0$ or $F = 1$) are considered. From the results shown in Table I, in the lowest energy state, F has the opposite polarization of A (B). Therefore, this circuit acts as an INV.

Coplanar Crossing. The coplanar crossing circuit consists of a a binary wire that crosses an inverter chain on the same planar layout. As depicted in Figure 8(f). A is the input of the vertical wire (the inverter chain), while B is the input of the horizontal wire (i.e., the binary wire). If A and B are fixed, the remaining three cells will have a polarization state that minimizes the total energy. Assume $A = 1$, $B = 1$, all possible energy states are shown in Table I. The lowest energy state is $F1 = 1, F2 = 1$. By symmetry, the lowest energy state can be determined for the other input combinations. In all cases, the lowest energy state corresponds to the desired signal crossing state. Therefore, it can, be concluded that in this model, two wires can cross each other with no interference, that is, the coplanar crossing correctly works.

Majority Voter. If the MV (majority voter) has three identical inputs, the lowest energy state corresponds to the condition in which the device cell and the output cell have the same polarization as the inputs. The energy is calculated for the case in which the MV has inputs $A = 1$, $B = C = 0$, as shown in Figure 8(g). The device cell D and the output cell F will settle in a state such that the overall energy is minimized. The four possible energy states are shown in Table I. The lowest energy state is the state in which the device cell $D = 0$ and the output cell $F = 0$. This corresponds to the desired MV function. The lowest energy state of other input combinations can be calculated similarly. In all cases, the lowest energy state corresponds to the state in which the device and the output cells are the majority of the inputs. Under the proposed model, the MV operates correctly.

To verify the validity of the proposed mechanical model, its steady state energy results were compared with those obtained through a computation-based model, such as QCADesigner [Walus et al. 2003]. Such comparison is valid because the proposed model and QCA both use Coulombic force for the inter-cell interactions and they can both be expressed as electric quadrupoles. So the same energy states are expected to occur in both of them, as corresponding to equivalent characterizations (e.g., cell size, cell distance, and amount of electric charge). So both QCA and the mechanical model should have the same ground state, represent the same logic and compute the same result. In all previous presented cases, the steady state analysis above yields the

same result as the simulation result of QCADesigner. This shows that the proposed model is complete as it can be used to characterize the steady state behavior of all QCA circuit primitives, including logic gates and interconnect structures.

Therefore, after computing the energy states of different circuits of mechanical cells, the same circuits have been also assembled with QCA cells and simulated by employing QCADesigner [Walus et al. 2003]. It has been verified that the simulation results of each and every logic device in QCADesigner are the same as the *ground state* (the state with the lowest energy) of its counterpart version in the proposed mechanical model. As both of these models utilize quasi-adiabatic clocking, then the cells stay in the ground state after switching. The agreement between simulated and computed results further confirms the validity of the proposed model for QCA. Moreover, as the devices evaluated previously constitute the basic components for building large QCA systems, the proposed model can be utilized with confidence.

4. ENTROPY AND DISSIPATION ANALYSIS

4.1 Operation of the Mechanical Cell

Bennett [2000] has concluded that three types of a physical reversible computing model are possible: (a) Ballistic, (b) Brownian, and (c) Clocked Brownian models. *Ballistic models* need isolation between the computational system and thermal noise. In *Brownian models*, the information-bearing degrees of freedom are strongly coupled to the non-information-bearing ones. In *clocked Brownian models*, the information-bearing degrees of freedom are locked and driven by the degree of freedom of a master clock, in addition to its coupling with other degrees of freedom (as in a normal Brownian model). The proposed model is a clocked Brownian model. The angular position of the rotation unit is the information-bearing degrees of freedom. It is locked and driven by the position of the sleeve. Thermal noise provides the lower bound for the energy needed to encode information (i.e., the energy involved, not the energy dissipated) in a clocked Brownian machine. When the mechanical cell is in the LOCK phase, the energy barrier separating the two possible states (also referred to as polarizations) must be bigger than kT (where T is the operating temperature and k is Boltzmann's constant); this ensures that the probability of overcoming the barrier is small enough for reliable storage of information. Also, in the SWITCH phase for a cell to reliably acquire a specific state, the driver must be strong enough to constrain the rotation angle (given by β) of the rotation unit, so that its change will not exceed 90° due to thermal noise. However, the dissipation of a clocked Brownian reversible machine is proportional to the speed of computing [Bennett 2000], but it is not limited by such bound. If the process is slow enough to be in *quasi-equilibrium*, then the machine is capable of computing with virtually no dissipation.

Consider the entropy and dissipation in the different operations of the proposed mechanical computing cell. The analysis of the entropy is difficult if each of the three states (*NULL*, 1, 0) is defined as corresponding to a specific position

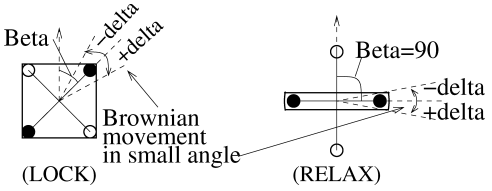

Fig. 9. Rotation unit with Brownian movement at a small angle.

of the rotation unit. In such a case, this will disable the Brownian movement of the rotation unit. A fixed rotation unit makes its changing range in angular position to zero, hence when calculating ΔS, the ratio of W_f and W_i becomes zero too. The definition of the *NULL*, 1 and 0 states must be modified so that the rotation unit can have a Brownian movement within a small angle interval given by $[-\delta, \delta]$ (Figure 9). Let S_0 denote the entropy of a cell in the *NULL* state.

The following analysis assumes a clocking unit (sleeve movement), that can store energy (a large, but still finite amount) and exchange energy with the mechanical cell with no loss of energy (this feature is not related to computing, hence it does not affect the analysis).

—First, in the mechanical model the cell is moved from the *NULL* state to either the 1, or 0 state reversibly. A driver and the movement of the sleeve can achieve this process. With no loss of generality, we consider the 1 state in this example. Initially, the shape of the cross section of the sleeve is changed to a circle. During this change, $W = -kT \log_2 \frac{\gamma}{2\delta}$ of work is done to the rotation unit and the heat exchange is $Q = kT \log_2 \frac{\gamma}{2\delta}$ (heat flows from the environment to the rotation unit), where γ is the range of the possible positions of the rotation unit. The driver must be strong enough to limit the rotation unit in $[0, 90]$ with a high probability, i.e., $\gamma < 90$. Subsequently, the shape of the cross section of the sleeve is changed to a square. During this process, $W = kT \log_2 \frac{\gamma}{2\delta}$ of work is exerted to the rotation unit and $Q = -kT \log_2 \frac{\gamma}{2\delta}$ (heat flows from the rotation unit into the environment).

This process is logically reversible: given the same initial state (i.e., *NULL*), then the cell goes into a final state specified by the polarization of the driver. Also, this procedure entails no dissipation. The total heat exchange between the system and the environment is zero. Work is done by the driver, the clocking unit, and the rotation unit, but the total work is zero. Although the rotation unit performs zero work in total, some energy (given by E_{p1})[1] is transferred into the clocking unit; E_{p1} is the difference between the potential energy of the driver and a *NULL* state cell and the potential energy of the driver and a cell in a polarized (1/0) state.

—Next, if the polarization of a cell in the LOCK phase is known, then it is possible to place the cell to the *NULL* state (when the clock goes to the RELAX phase) with no dissipation. This process needs an external driver with the same polarization as the cell. Initially, when the shape of the cross section

[1]This energy initially comes by applying the driver.

of the (clocking unit) sleeve becomes circular, the external driver keeps the rotation unit in a range smaller than [0, 90]. During this step, $W = -kT\log_2 \frac{\gamma'}{2\delta}$ is exerted to the rotation unit and $Q = kT\log_2 \frac{\gamma'}{2\delta}$ (also, γ' is the range of possible positions of the rotation unit). The driver must keep $\gamma' < 90$. Subsequently, when the clock is in the RELAX phase, the state of the cell changes into *NULL*. During this process, $W = kT\log_2 \frac{\gamma'}{2\delta}$ and $Q = -kT\log_2 \frac{\gamma'}{2\delta}$. This process is also reversible and no heat is dissipated. There is an energy (given by E_{p2}) that is transferred from the clocking unit to the driver. E_{p2} is the difference between the potential energy of this driver and a *NULL* cell and the potential energy of this driver and a polarized cell.

Consider an entire clock period (from the RELAX phase to the LOCK phase and then back to the RELAX phase), so no energy dissipation will occur. From the RELAX phase to the SWITCH phase, the potential energy E_{p1} between the driver and the charged balls flows into the clocking unit. Then from the RELEASE to the RELAX phase, E_{p2} will flow back from the clocking unit and it becomes potential energy. E_{p1} and E_{p2} are established by the strength of the drivers during these two phases; thus, it is possible to find a *Carnot cycle* provided the strength of the driver is kept constant during these two phases; that is, $E_{p1} = E_{p2}$. If the strength of the driver is not constant, then $E_{p1} - E_{p2}$ will flow into the clocking unit.

The reversibility of this process depends on the polarization of the external driver during the RELEASE phase. The following scenarios can be distinguished:

1) If there is no driver during the RELEASE phase, then a free expansion will occur when the cross section of the sleeve changes to a circular shape: the rotation unit increases its range of possible angular positions from [0, 90] to [0, 180]. As in the ideal gas example presented previously, there is no work and exchange in free expansion. Prior to free expansion, $W = -kT\log_2 \frac{90}{2\delta}$ is done to the rotation unit and $Q = kT\log_2 \frac{90}{2\delta}$ (from the environment to the rotation unit). After the free expansion, $W = kT\log_2 \frac{180}{2\delta}$ and $Q = -kT\log_2 \frac{180}{2\delta}$. So, in the whole RELEASE phase, the clocking unit exerts $\sum W = kT$ of work to the rotation unit and the system dissipates kT ($\sum Q = -kT$).

2) If the driver's polarization is different from the cell, then energy dissipation will occur. As illustrated in Figure 10, the driver will force the balls to the other polarization state. In the LOCK phase, the polarization change cannot occur because there is not enough energy to compress the stick to turn the rotation unit to a new polarization. However, during the SWITCH phase, when the cross section of the sleeve is changing from a square to a circle, the energy required for the polarization change is small. At this point, the rotation unit will change into the new polarization; it will receive a kinetic energy E_k from this change and vibrate around the new polarization position until damping due to the air will slow it gradually to the average thermal noise level. Damping will cause dissipation of E_k. Prior to the polarization change, due to the driver, the angle β of the rotation unit is $[90 - \gamma_1, 90)$, where $0 < \gamma_1 < 90$. During the RELEASE phase prior to the polarization change, $W = -kT\log_2 \frac{\gamma_1}{2\delta}$ and $Q = kT\log_2 \frac{\gamma_1}{2\delta}$. Then, a free expansion process increases the possible range of β to

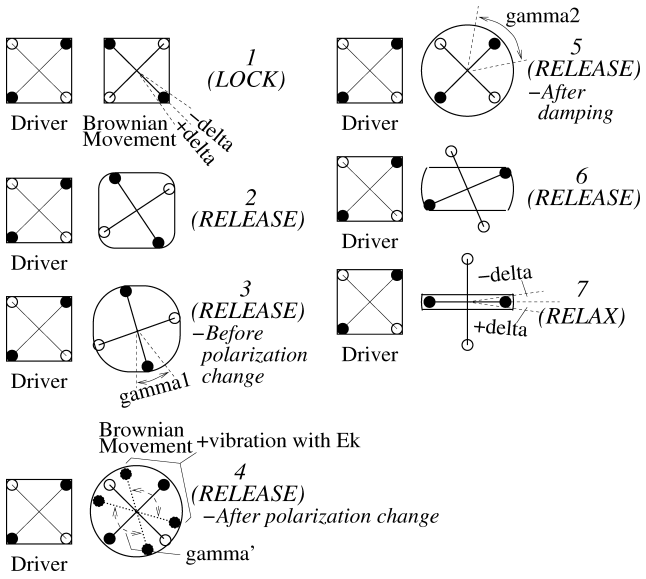

Fig. 10. RELEASE phase for acell under a driver of different polarization.

$\gamma' = min(90 + 2\gamma_1, 180)$. In free expansion, $W = 0$ and $Q = 0$. During damping, E_k is dissipated into the environment to slow down the rotation unit. Also, the driver finally limits the range of β at an angle γ_2. During this process, $W = kT \log_2 \frac{\gamma'}{\gamma_2}$ and the rotation unit receives $Q = -kT \log_2 \frac{\gamma'}{\gamma_2}$ from the environment. After damping till the end of the RELEASE phase, $W = kT \log_2 \frac{\gamma_2}{2\delta}$ and $Q = -kT \log_2 \frac{\gamma_2}{2\delta}$.

So, in the entire RELEASE phase, the total work is $\sum W = kT \log_2 \frac{\gamma'}{\gamma_1}$ and $E_k + kT \log_2 \frac{\gamma'}{\gamma_1}$ is dissipated (equal to $-\sum Q$). E_k, γ' and γ_1 are determined by the strength of the driver. As the driver is strong enough to set a cell to a polarization with high probability, then it must be in the order of kT (according to Boltzmann's distribution). Approximately, E_k is given by $E_k = kT$ as $\gamma' = min(90 + 2\gamma_1, 180)$ and $0 < \gamma_1 < 90$, $kT \log_2 \frac{\gamma'}{\gamma_1} \geq 2$. So, the RELEASE phase dissipates at least $2kT$.

3) If the polarization of the cell is not known in the LOCK phase, it is impossible to utilize any reversible process to set it to the *NULL* state. If a constant driver is applied, then there is a 50% probability of being in the same polarization as the cell, thus no energy is dissipated. However, there is also a 50% probability to be in the opposite polarization as the cell, thus at least $2kT$ will be dissipated. The expected dissipation is kT. If no external driver is applied, the process still dissipates $Q = kT$.

As suggested in Section 2.2, the "free expansion" process when resetting a computing cell with no knowledge of its state, is the source of the dissipation lower bound for information loss. In the analysis above, it is shown that releasing a QCA cell without a driver of equal polarization will result in "free expansion" and, in turn, dissipation.

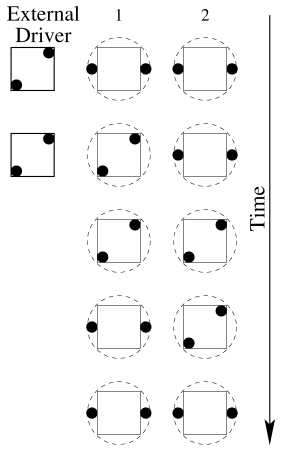

Fig. 11. A signal path with two cells.

4.2 Validation of Dissipation Analysis

In [Timler and Lent 2003; Lent et al. 2006], a quantitative calculation of the operation of several QCA circuits have been presented. The dissipation analysis is made on the same set of circuits as in [Timler and Lent 2003; Lent et al. 2006] using the proposed mechanical model.

Erasure of a single cell. The dissipation of setting and erasing a single cell has been calculated in Timler and Lent [2003]. It has been concluded that when utilizing a so-called Demon cell with same polarization as the cell being erased, the erasure process has dissipation less than $kT \ln 2$. When no such "Demon cell" exists, dissipation is larger than $kT \ln 2$. This agrees with the results of Section 4.1: at least $kT \ln 2$ will be dissipated if a stand-alone cell is erased, however if a cell of same polarization is present to drive the cell during the RELEASE phase, then dissipation can be avoided.

Two-cell signal path. Two cells in adjacent clocking zones constitute the simplest circuit under the proposed model (Figure 11). Over five clocking phases, its operation is as follows:

1) Initially, cells 1 and 2 are both in the *NULL* state, with clocking in the RELAX phase. An external driver is applied to cell 1. With no loss of generality, assume that the driver's value is 1.

2) Cell 1 goes through the SWITCH phase. As described in Section 4.1, cell 1 has a polarization of 1; the potential energy (E_p) between the driver and cell 1 (denoted as E_d) and the energy between cell 1 and cell 2 (denoted by E_1) are transferred into the clocking unit.

3) Cell 1 goes into the LOCK phase and the external driver is removed. Meanwhile, cell 2 acquires the value 1. The potential energy between cell 1 and cell 2 ($E_p = E_2$) is transferred into the clocking unit.

4) Cell 1 is placed in the RELEASE phase under the bias of cell 2, which is now in the LOCK phase. As described in Section 4.1, cell 1 is under a same polarization condition of bias, so no explicit dissipation occurs; E_2 comes from the clocking unit and becomes potential energy between cell 1 and cell 2.

5) Cell 2 is placed in the RELEASE phase under no bias, so at least Tk of energy is drained from the clocking unit and dissipated. The clocking unit also provides E_1 as potential energy between cell 1 and cell 2.

Over the entire cycle of the circuit, the external driver provides E_d energy. At least kT of this energy is dissipated and the remaining energy goes into the clocking unit. A two-cell signal path operates as the "one test cell plus one demon cell" described in Timler and Lent [2003]. The mechanical model leads to the same conclusion as calculated in Timler and Lent [2003]: the first cell works reversibly, because the second cell works as a demon cell; the erasure of the second cell is irreversible because when it is released there is no demon cell for it.

Shift Register with One Cell per Stage (SR1): The shift register with one cell per stage (denoted as SR1) can be viewed as the multiple concatenation of two-cell signal paths, as analyzed previously. As illustrated in Figure 12, cell m receives its logic value from cell $m-1$. When cell $m-1$ is in the RELAX phase, at the same time cell $m+1$ is in the SWITCH phase with the same value of cell m. Then, cell m is in the RELAX phase, while the signal is delivered to cell $m+2$. The distance between the centers of two adjacent cells is denoted by d. When a cell (except for the first and last cells in the line of the shift register) is in the SWITCH phase, then it is driven by the cell located prior to it. When it is in the RELAX phase, then it is driven by the cell located after it. As proven previously, this behavior of the cells is reversible.

For a shift register with n stages, its operation consists of $n+2$ phases. All stages (except the last one) work reversibly as described in section 4.1. After passing one bit information through SR1, the circuit receives E_d (as defined in the analysis for a two-cell signal path) from the driver, among which kT is dissipated and the rest of the energy goes into the clocking unit. kT dissipation is the result of an information loss at cell n. If the output of SR1 is connected to another circuit, then the information propagates into the next circuit and cell n is released under the driving of that circuit. In this case, no dissipation will occur in SR1. As driver, SR1 provides energy to the next circuit, just as it receives energy from its driver. If SR1, its driver and the next circuit have the same design parameters (cell size, distance and charge quantity), then SR1 will provide the next circuit with the same amount of energy of E_d. Timler and Lent [2003] and Lent et al. [2006] have treated SR1 as a chain of "demon" cells; their calculation has confirmed that the energy dissipated per cell per clock switching can be much less than $kT \ln 2$.

The dissipation analysis in the proposed model takes into consideration the energy exchange with the clocking system. The clocking system operates like the moving-wall in the gas model of Section 2.2; it provides or absorbs energy from the computing system during the different phases of the working-cycle, thus making possible to balance the total work in the reversible process.

4.3 Energy Dissipation Analysis of Circuit Units

In this section, the entropy change and energy dissipation of various QCA circuits are analyzed. In the analysis presented in this section, it is assumed that

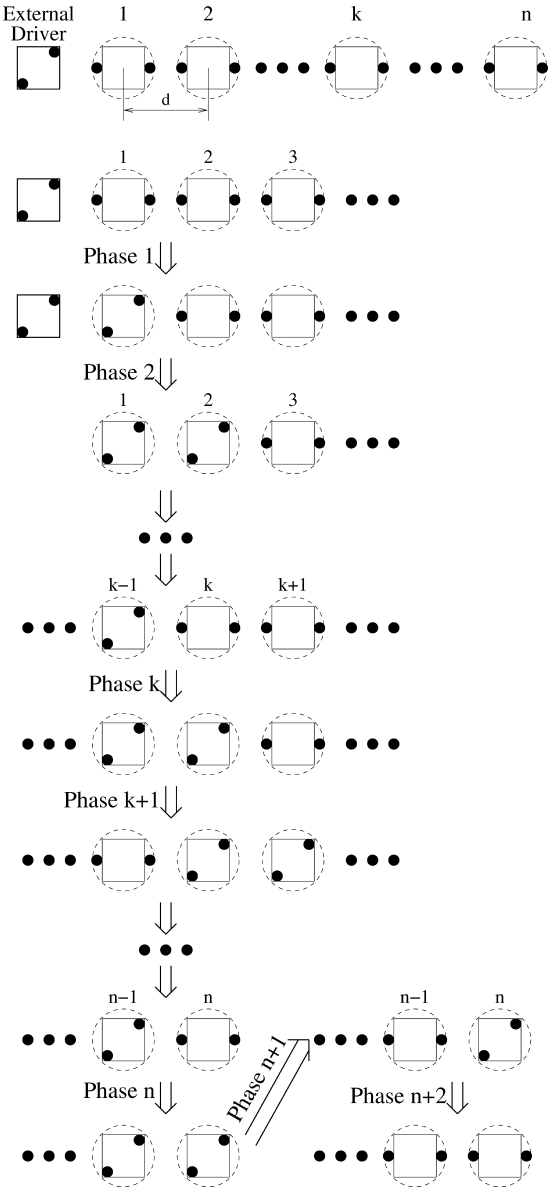

Fig. 12. Shift register with one cell per stage (SR1).

the parameters (q and a) of the device are selected such that the strength of the driver for each cell is sufficiently strong (as discussed previously in Section 4.1). For ease of presentation, only negative charged balls in the cell are presented in the figures of this section.

Shift Register with Multiple Cells per Stage (SR2). For a register whose stages consist of different numbers of cells (SR2), the non-dissipation feature also applies. When the kth stage is in the SWITCH phase, its cells are driven by

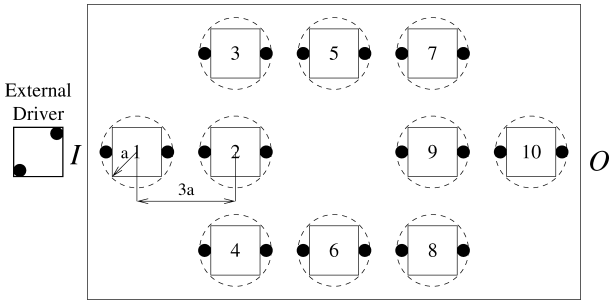

Fig. 13. Fanout and reversible eraser.

the $(k-1)$th stage. When it is in the RELEASE phase, its cells are driven by the $(k+1)$th stage. So, as in SR1, the first $n-1$ stages in a n stage shift register work reversibly. If SR2 does not drive other circuits, each cell in its last stage will dissipate kT energy. If it drives other circuits, the entire SR2 works reversibly and does not dissipate any energy.

Fanout Circuit. For a fanout (Figure 13), every cell inside the circuit is operated reversibly, too. However, there are two output cells, and they have no interaction with each other. So, if they are in the RELEASE phase without driving a subsequent circuit, the dissipation is $2kT$, twice as much as the dissipation of a single cell. If both outputs transfer information to subsequent circuits and are in the RELEASE phase while driving these circuits, then the fanout circuit is reversible. As a result, the fanout-then-erase circuit of Figure 13 is reversible. The eraser (cells 5 to 8) does not destroy information. Its inputs come from the fanout and can only take "00" or "11" as values. So, any input combination carries only one bit of information. The cell that erases two copies of information into one, operates as discussed in Section 4.1. It is reversible because it has the same polarization driver in the SWITCH and RELEASE phases. The driver strengths in the two phases are different, $E_{p1} = 2E_d$, $E_{p2} = E_d$, so $E_{p1} - E_{p2} = E_d$ will flow into the clocking unit. This conclusion can be extended to the n-to-1 reversible erasure, that is, $(n-1)E_d$ energy flows into the clocking unit.

This analysis shows that the fanout structure by itself does not necessarily result in energy dissipation. In comparison with the normal connection (shift register), the increase of dissipation is associated with the erasure of an extra output cell. This conclusion holds also for the generic case of a one-to-n fanout circuit ($n \geq 2$).

Inverter. From the steady state energy calculation, it has been shown that the two input cells of the three-cell inverter are in the RELEASE phase under a same-polarization driver. So, only the output cell in the three-cell inverter dissipates an energy of kT when released and with no transfer of information to a subsequent circuit. If the three-cell inverter connects to another circuit, then the output cell operates reversibly, too.

The inverter in Figure 14 consists of an 1-to-2 fanout circuit and a three-cell inverter. So, it is also reversible.

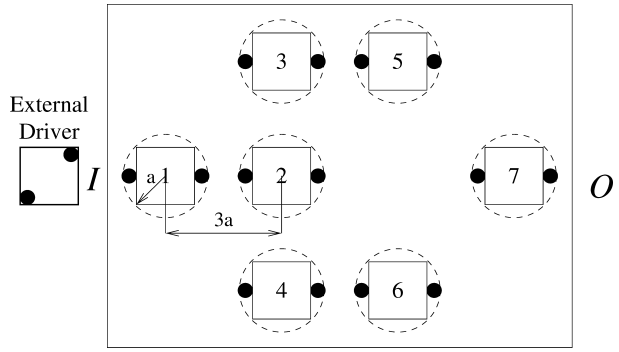

Fig. 14. One-input one-output inverter as one-to-two fanout and three-cell inverter.

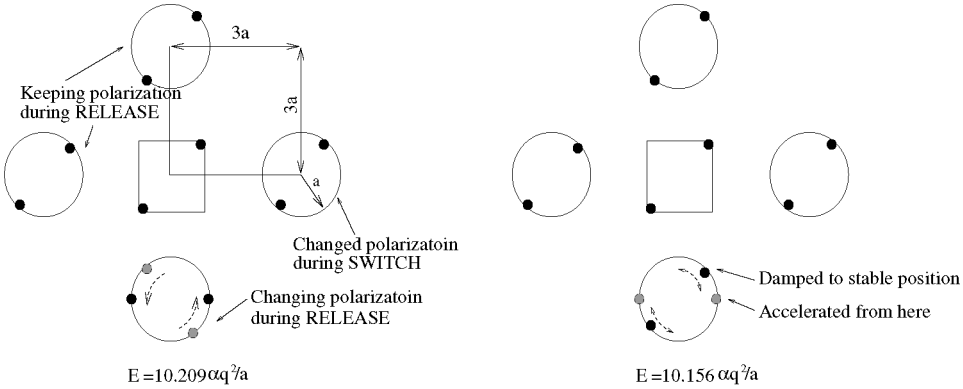

(a) Before damping (b) After damping

Fig. 15. Damping in Majority Voter causes dissipation.

Majority Voter. In the MV, if the inputs are 111 or 000, then no free expansion or damping will occur. The energy change is the same as the reversible erasure in the previous analysis. The voter cell erases 2 bit information reversibly and $2kT$ of energy goes into the clocking unit. If the input values are one of the remaining six possible combinations, then the input cell with the minority input will dissipate $kT + E_d$ energy when released under an opposite polarization driving condition (as shown in Figure 15). E_d must be at least kT to ensure that the model operates reliably. Overall, at least $2kT$ energy is dissipated during the RELEASE phase.

So, there is 25% probability that the MV gets equal valued inputs and erases two bits of information reversibly. This does not dissipate energy directly, but an energy of $2kT$ goes into the clocking unit and will be finally dissipated into the environment to keep a stable clocking. There is 75% probability that the MV dissipates an energy of $2kT$ into the environment. Hence, the MV dissipates $2kT$ heat on average; due to loss, each input combination contains $-k \log_2 \frac{1}{8}$ of information, and each output contains only $-\log_2 \frac{1}{2}$ of information. Therefore, two bits of information are destroyed in the MV and at least $2kT$ of heat must be

dissipated. This dissipation is a lower bound imposed by logical irreversibility and it is in agreement with the expected dissipation as found from the above calculation.

5. LANDAUER AND BENNETT CLOCKING SCHEMES

The clocking scheme that was assumed in the previous sections, is generally referred to as *Landauer clocking*. Landauer clocking is the scheme utilized in almost all previous QCA papers found in the technical literature. Landauer clocking is simple, however, it makes few circuits (such as the MV) to be irreversible and dissipative. In Timler and Lent [2003] and Lent et al. [2006], a different scheme (i.e., the so-called *Bennett clocking*) has been proposed for QCA, under which MV can be nondissipative. Figure 16 illustrates these two types of clocking scheme. The proposed model can be used to understand the operations of the two clocking schemes. An analysis and comparison of the two clocking schemes are presented in this section.

The basic principle of Bennett clocking is that the bit information is held in place by the clock until an operation is completed by the circuit [Lent et al. 2006]. Then, it is erased in the reverse order of computation, as illustrated in Figure 16(b). Thus, every cell is switched and released when all other cells in the circuit are in the same configuration. It is evident that every cell has a driver of same-polarization when it is released. As per the conclusions drawn in Section 4.1, every cell works reversibly. So, the computing process of the whole circuit is reversible. Quantum-dynamic calculation has shown that energy dissipation per switching event is much less than $kTln2$ for QCA circuits containing the MV and fan-out [Lent et al. 2006]. Bennett clocking does not require any change in QCA layout, because only the clocking signals are modified.

However, the control of Bennett clocking is more complex compared with Landauer clocking. Additionally, in Bennett clocking the next operation cannot begin until the circuit is released from the output to the input. For QCA, the speed of a Bennett clocked computation is proportional to the timing depth (number of clocking zones) of the circuit. By comparison, Landauer clocking releases a cell after four phases (1 clock cycle) of quasi-adiabatic switching, so that the cell can be used in the next operation. Landauer clocking leads to a pipeline implementation (Figure 16) and an increase in computing speed. Bennett clocking releases the cells from output to input, so the last cell is locked; as for the input cells, they are released under no driver. As analyzed in previous sections, the only energy dissipation in Bennett clocking occurs when the input cells are released under no driver.

A two-to-one multiplexer (MUX) is used as an example to illustrate the advantages and disadvantages of Landauer and Bennett clocking schemes. The schematic diagram and the corresponding layout of the MUX are shown in Figure 17; when $Sel = 1$, $F = A$; when $Sel = 0$, $F = B$. The clocking zone assignments are the same for Landauer and Bennett clocking schemes and are represented by different shaded colors and patterns in the layout. The timing diagrams for Laudauer and Bennett clocking schemes are depicted in Figure 18.

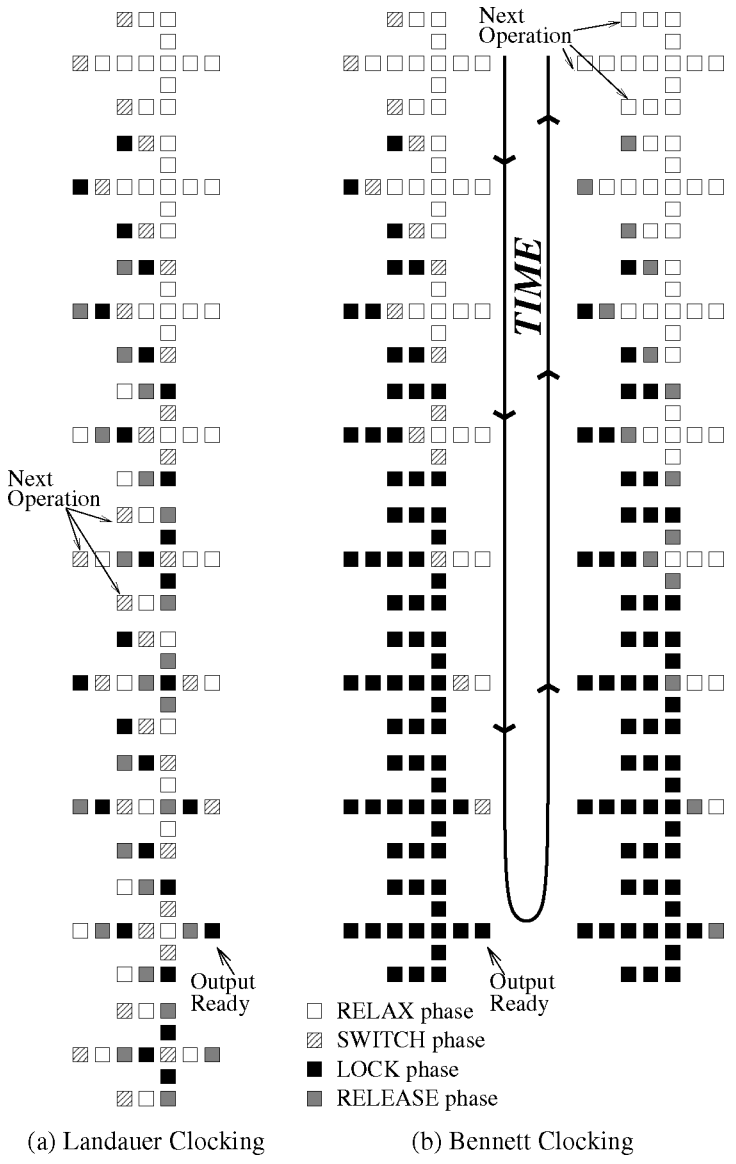

Fig. 16. Landauer and Bennett clocking schemes.

—If Landauer clocking is used, the delay between the inputs and the outputs is 10; consecutive inputs can be applied at every clock cycle (4 clocking zones). So, consecutive outputs are produced every clock cycle.

—With Bennett clocking, the delay between inputs and outputs is again 10 clocking zones. However, consecutive inputs can be applied with a delay of 22 clocking zones, which is 4 times more than for Landauer clocking.

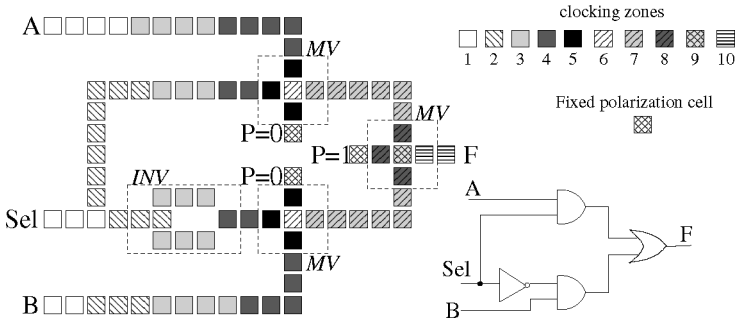

Fig. 17. Two-to-one MUX schematic and layout diagrams.

Bennett clocking results in a longer delay compared with Landauer clocking; however, the energy dissipation of Bennett clocking occurs only at the input/output ports and the internal energy dissipation of Bennett clocking can be made arbitrarily small. The energy dissipation of Landauer clocking is proportional to the number of irreversible gates in the circuit. Therefore, Bennett clocking is more energy efficient than Landauer clocking. Clearly, there is a trade off between power (and reversible computing) and delay (for high performance computing) when choosing the desired clocking scheme for a QCA implementation.

6. CONCLUSION

This paper has presented a new mechanical-based model that is amenable to QCA operation and computation. This mechanical model is inspired by the operational features of clocked molecular QCA to provide an intuitive and classical view of the energy and heat phenomena. The proposed mechanical model consists of a sleeve of changing shape; four electrically charged balls (two with negative charge and two with positive charge) are used to model the electrically neutral QCA molecule. The balls are connected by a stick that rotates around an axle in the sleeve. The sleeve acts as a clocking unit, while the angular position of the stick within the changing shape of the sleeve, identifies the phase for quasi-adiabatic switching. Recently, QCA has been advocated as a potential candidate technology for implementing reversible computing, so the proposed model can be utilized to assess these features. By avoiding a full quantum-thermodynamical calculation, it has been shown that the proposed model is versatile in evaluating different features (such as energy consumption for reversible computing and clocking schemes) at device and circuit levels for molecular QCA implementation.

The steady state energies of various QCA devices have been calculated using the proposed model. It has been shown that the mechanical model agrees with the operation of all basic QCA devices. These results have been also confirmed by QCADesigner. The proposed model has been used to characterize the dynamic behavior of QCA circuits. It has been shown that this model is very effective in analyzing different QCA circuits for reversible computing.

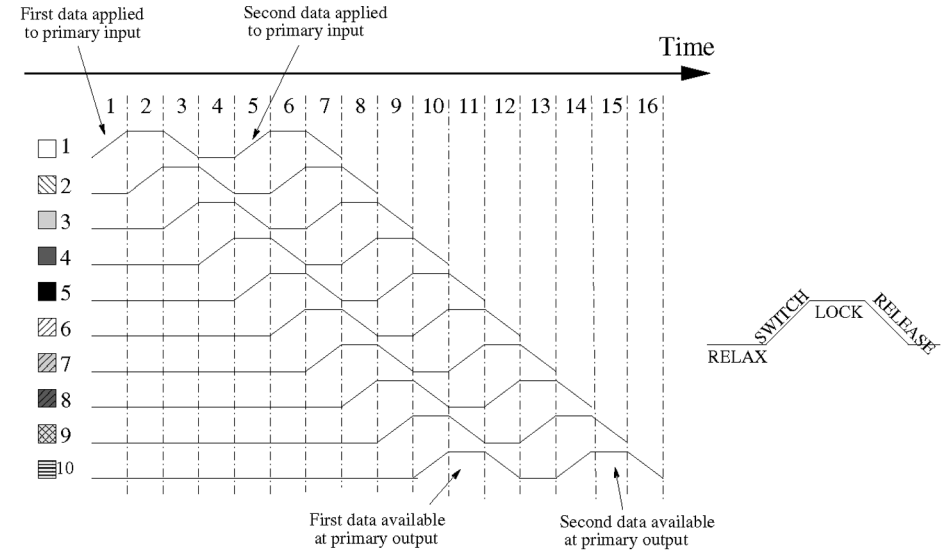

(a) Timing of Landauer clocking scheme

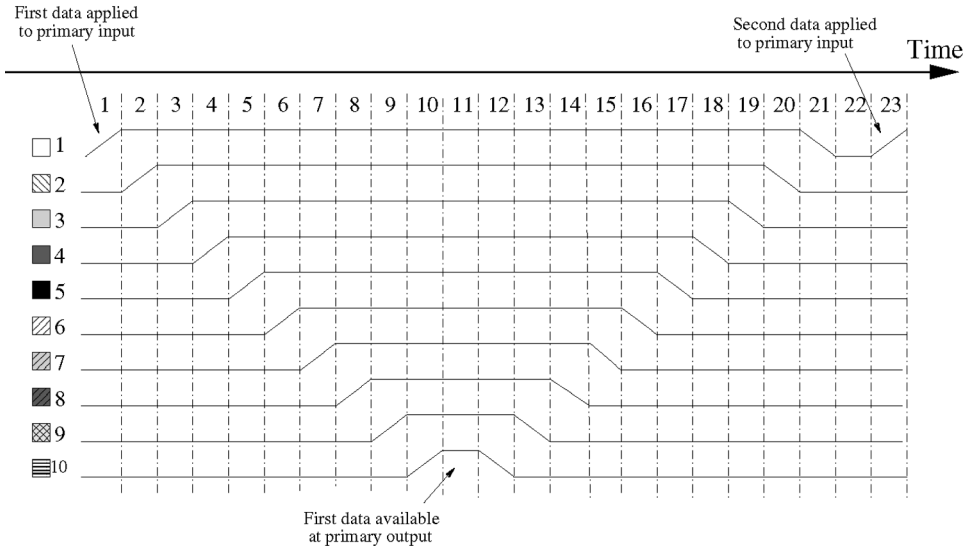

(b) Timing of Bennett clocking scheme

Fig. 18. Timing Diagrams for the MUX under Landauer and Bennett clocking schemes.

—The QCA shift register (irrespective of the number of cells per stage) is a reversible circuit.

—Differently from other technologies, the fanout circuit in QCA does not necessarily result in energy dissipation; the increase in dissipation is the result of having an additional output cell connected to this circuit. Therefore,

dissipation is associated with the irreversible release at the output cells and the reversibility of adjacent circuits.

—The 3-cell inverter is a reversible circuit.

—The majority voter circuit in QCA shows an energy dissipation dependency on the clocking scheme; MV is irreversible if Landauer clocking is used, but reversible under Bennett clocking. This confirms previous results found in the technical literature [Lent et al. 2006].

—Through the example of a two-to-one multiplexer, this paper has confirmed that there is a tradeoff between energy consumption (and therefore reversible computing) and the number of clocking zones (delay) when selecting a clocking scheme for QCA.

REFERENCES

Amlani, I., Orlov, A. O., Toth, G., Lent, C. S., Bernstein, G. H., and Snider, G. L. 1999. Digital logic gate using quantum-dot cellular automat. *Science 284* (5412), 289–291

Antonelli, D. A., Chen, D. Z., Dysart, T. J., Hu, X. S., Kahng, A. B., Kogge, P. M., Murphy, R. C., and Niemier, M. T. 2004. Quantum-dot cellular automata (qca) circuit partitioning: problem modeling and solutions. In *Proceedings of the Design Automation Conference (DAC)*. 363–368.

Bennett, C. H. 1973. Logic reversibility of computation. *IBM J. Res. Dev. 17*, 525–532.

Bennett, C. H. 2000. Notes on the history of reversible computation. *IBM J. Res. Dev. 44*, 44, 525–532.

Compano, R., Molenkamp, L., and Paul, D. J. 2003. Technology roadmap for nanoelectronics. *European Commission IST Programme, Future and Emerging Technologies*. www.itrs.net/Links/2003ITRS/LinkedFiles/ERD/NanoeletronicsRdmp.pdf

Dimitrov, V. S., Jullien, G. A., and Walus, K. 2002. Quantum-dot cellular automata carry-look-ahead adder and barrel shifter. In *Proceedings of the IEEE Emerging Telecommunications Technologies Conference*. 2/1–2/4.

Fermi, E. 1956. *Thermodynamics*. Dover Publications Inc., New York, NY.

Fredkin, E. and Toffoli, T. 1982. Conservative logic. *Int. J.Theor. Phys. 21*, 219–253.

Frost, S. E., Rodrigues, A. F., Janiszewski, A. W., Rausch, R. T. and Kogge, P. M. 2002. Memory in motion: A study of storage structures in QCA. In *Proceedings of the Workshop on Non-Silicon Computation*.

Hu, W., Sarveswaran, K., Lieberman, M., and Bernstein, G. H. 2005. High-resolution electron beam lithography and DNA nano-patterning for molecular QCA. *IEEE Trans. Nanotech. 4*, 3, 312–316.

Huang, J., Ma, X., and Lombardi, F. 2006. Energy analysis of QCA circuits for reversible computing. In *Proceedings of the 6th IEEE Conference on Nanotechnology (NANO)* 1, 39–42.

Huang, J., Momenzadeh, M. Schiano, L., and Lombardi, F. 2005. Simulation-based design of modular QCA circuits. In *Proceedings of the 5th IEEE Conference on Nanotechnology 2*, 533–536.

Huang, J., Momenzadeh, M., Schiano, L., Ottavi, M., and Lombardi, F. 2005. Tile-based QCA design using majority-like logic primitives. *ACM J. Emerg. Technol Comput. Syst. 1*, 3, 163–185.

Huang, J., Momenzadeh, M., Tahoori, M., and Lombardi. F. 2005. On the evaluation of scaling of QCA devices in the presence of defects. *IEEE Trans. Nanotech 4*, 6, 740–743.

Landauer, R. 1961. Irreversibility and heat generation in the computing process. *IBM J. Res. Dev. 5*, 183–191.

Lent, C. S., Liu, M., and Lu, Y. 2006. Bennett clocking of quantum-dot cellular automata and the limits to binary logic scaling. *Nanotech. 17*, 16, 4240–4251.

Lent, C. S. and Tougaw, P. D. 1997. A device architecture for computing with quantum dots. In *Proceedings of the IEEE 85*, 4, 541–557.

Lent, C. S., Tougaw, P. D., and Porod, W. 1994. Quantum cellular automata: the physics of computing with arrays of quantum dot molecules. In *Proceedings of the Workshop on Physics and Computing*, 5–13.

MA, X., HUANG, J., METRA, C., AND LOMBARDI, F. 2005. Testing reversible 1D arrays of molecular QCA. In *Proceedings of the IEEE International Symposium on Defect and Fault Tolerance in VLSI Systems (DFT)*. 71–79.

NIEMIER, M. T. AND KOGGE, P. M. 1999. Logic-in-wire: using quantum dots to implement a microprocessor. In *Proceedings of the International Conference on Electronics, Circuits, and Systems (ICECS)* 3, 1211–1215.

NIEMIER, M. T. AND KOGGE, P. M. 2001. Problems in designing with QCAs: layout=timing. *Int. J. Circ. Theory Appl. 29*, 1, 49–62.

NIEMIER, M. T., KONTZ, M. J., AND KOGGE, P. M. 2000. A design of and design tools for a novel quantum-dot based microprocessor. In *Proceedings of the ACM Design Automation Conference (DAC)*. 227–232.

NIEMIER, M. T., RODRIGUES, A. F., AND KOGGE, P. M. 2002. A potentially implementable FPGA for quantum dot cellular automata. In *Proceedings of the 1st Workshop on Non-Silicon Computation (NSC-1)*. Held in Conjunction with the *8th International Symposium on High Performance Computer Architecture (HPCA)*.

OTTAVI, M., MOMENZADEH, M., AND LOMBARDI, F. 2005. Modeling QCA defects at molecular level in combinational circuits. In *Proceedings of the IEEE International Symposium on Defect and Fault Tolerance in VLSI Systems (DFT)*. 208–216.

SMITH, C. G. 1999. Computation without current. *Science 284*, 2, 274.

TAHOORI, M., MOMENZADEH, M., HUANG, J., AND LOMBARDI, F. 2004. Testing of quantum cellular automata. *IEEE Trans. Nanotechn. 3*, 4, 432–442.

TANG, R., ZHANG, F., AND KIM, Y. B. 2005. QCA-based nano circuits design. In *Proceedings of the IEEE International Symposium on Circuits and Systems*. Kobe, Japan, 2527–2530.

TANG, R., ZHANG, F., AND KIM, Y. B. 2005. Quantum-dot automata SPICE macro model. In *Proceedings of the ACM Great Lakes Symposium on VLSI*. Chicago, IL, 108–11.

TIMLER, J. AND LENT, C. S. 2003. Maxwell's demon and quantum-dot cellular automata. *J. Appl. Phys. 94*, 2 1050–1060.

TOFFOLI, T. 1980. Reversible computing. Tech. Rep. MITLCSTM151, MIT Laboratory for Computer Science.

TOTH, G. 2000. Correlation and coherence in quantum-dot cellular automata. Ph.D. Thesis, University of Notre Dame.

TOUGAW, P. D. AND LENT, C. S. 1994. Logical devices implemented using quantum cellular automata. *J. Appl. Phys. 75*, 3, 1818–1825.

TOUGAW, P. D. AND LENT, C. S. 1996. Dynamic behavior of quantum cellular automata. *J. Appl. Phys. 80*, 15, 4722–4736.

WALUS, K., BUDIMAN, R. A., AND JULLIEN, G. A. 2002. Effects of morphological variations of self-assembled nanostructures on quantum-dot cellular automata (QCA) circuits. *Frontiers of Integration, An International Workshop on Integrating Nanotechnologies*,

WALUS, K., DYSART, T., JULLIEN, G. A., AND BUDIMAN, R. A. 2003. QCADesigner: A rapid design and simulation tool for quantum-dot cellular automata. In *Proceedings of the 2nd International Workshop on Quantum Dots for Quantum Computing and Classical Size Effect Circuits*. Notre Dame, IN.

WALUS, K., DYSART, T., JULLIEN, G. A., AND BUDIMAN, R. A. 2004. QCADesigner: A rapid design and simulation tool for quantum-dot cellular automata. *IEEE Trans. Nanotech. 3*, 26–29.

WALUS, K., VETTETH, A., JULLIEN, G. A. AND DIMITROV, V. S. 2003. RAM design using quantum-dot cellular automata. In *Proceedings of the Nanotechnology Conference*. 2, 160–163.

Received August 2006; revised February 2007; accepted May 2007